catalysts

MDPI

Article

Physico-Chemical Changes in the KCl-$MgCl_2$/La-FAU Composite Catalyst Induced by Oxidative Dehydrogenation of Ethane

Mehran Sajad [1,*], Roman Bulánek [1] and Stanislav Šlang [2]

[1] Department of Physical Chemistry, Faculty of Chemical Technology, University of Pardubice, Studentska 573, 532 10 Pardubice, Czech Republic; Roman.Bulanek@upce.cz
[2] Center of Materials and Nanotechnologies, Faculty of Chemical Technology, nám. Čs. Legií 565, University of Pardubice, 532 10 Pardubice, Czech Republic; stanislav.slang@upce.cz
* Correspondence: Mehran.Sajad@student.upce.cz; Tel.: +420-777956079

Abstract: In this research, a binary eutectic composition of KCl and $MgCl_2$ supported over lanthanum exchanged FAU (faujasite) zeolite has been investigated for the oxidative dehydrogenation (ODH) of ethane. The catalyst was prepared by the thermal treatment of La-FAU with a mechanical mixture of alkali chlorides under a flow of helium at 500 °C. The eutectic mixture of alkali chlorides formed at this temperature and a molten layer were spread over the support. Synthesized fresh and spent catalysts were characterized to obtain information about changes in crystallinity, textural properties, phase content, chemical composition, and morphology of the catalyst over the reaction time. The initial conversion of ethane was 80% with ethene as the main product (65% yield). The catalyst deactivation has been demonstrated over time on the stream (TOS). The characterization methods confirmed that the chlorine was being removed from the catalyst. The side products detected by mass spectroscopy, including chlorinated hydrocarbons, have been found as a key pathway of chlorine removal from the catalyst. The exchange of chlorine for oxygen in the catalyst led to a significant decrease in the activity and production of higher hydrocarbons and their oxygenates as side products of the ODH reaction.

Keywords: oxidative dehydrogenation; alkali chlorides; ethane; ethylene

check for updates

Citation: Sajad, M.; Bulánek, R.; Šlang, S. Physico-Chemical Changes in the KCl-$MgCl_2$/La-FAU Composite Catalyst Induced by Oxidative Dehydrogenation of Ethane. *Catalysts* **2021**, *11*, 392. https://doi.org/10.3390/catal11030392

Academic Editor: Changzhi Li

Received: 25 February 2021
Accepted: 16 March 2021
Published: 19 March 2021

Publisher's Note: MDPI stays neutral with regard to jurisdictional claims in published maps and institutional affiliations.

Copyright: © 2021 by the authors. Licensee MDPI, Basel, Switzerland. This article is an open access article distributed under the terms and conditions of the Creative Commons Attribution (CC BY) license (https://creativecommons.org/licenses/by/4.0/).

1. Introduction

Currently, ethene is mainly produced by cracking of naphtha, as one of the main feedstocks for petrochemistry, whereas due to the depletion of fossil fuels and the global demand growth for this olefin [1,2], it is necessary to find a new pathway for the efficient production of ethene. Ethane, a significant by-product of cracking processes that accompanies the production of its olefin, is mainly implemented as fuel due to its lower reactivity, albeit oxidative dehydrogenation is a thermodynamically accessible route to convert this alkane into more valuable olefin. ODH has advantages compared to its non-oxidative competitor that makes it very attractive, comprising the fact that ODH reaction is exothermic and not equilibrium limited [2–6].

Several catalytic systems have been studied in oxydehydrogenation reactions in recent decades. Among the systems that attract the most attention are supported or mixed oxides (mainly vanadium-, molybdenum-, phosphorus, or boron-based ones) [7–9], metal-free carbon-based [10], and chloride-based materials [5,11]. Concerning the last group, it was first found that the addition of a small amount of chlorine or organochlorides to the gas phase significantly affects the activity and selectivity of the oxydehydrogenation reactions over the oxide catalysts [12]. These additives mainly affected the structure of the catalyst surface—the interaction of chlorinated hydrocarbons or chlorine with the surface produced chlorides, which modified the properties of the active centers of the

catalyst. Furthermore, the radical species generated by the assistance of chlorine could influence the rate of the reaction. Later, it was shown that supported chloride catalysts are one of the promising candidates for oxidative dehydrogenation of light alkanes to olefins [6,13–27]. The advantage of using a mixture of molten salts is the ability to work in a wide temperature range if the salts make eutectics that melt at low temperatures [27,28].

Different explanations were stated to illustrate the reasons for the higher activity and selectivity caused by the presence of alkali chlorides. For instance, it was suggested that the alkali chlorides applied to different zirconia-based catalysts and metal oxides (for instance, MgO, TiO_2, SiO_2, and Dy_2O_3/MgO) provide a dynamically rearranging reaction interface and therefore create new sites and increase the number of active sites for ODH [5,6,14,16,18,24,25,27,29]. Hypochlorite (OCl^-) has been suggested frequently as the active species on the surface of the overlayer in supported alkali chloride catalysts [6,8,16,24,27,29]. The mechanism proposed by Lercher et al. (based on a study of LiCl/MgO/Dy_2O_3 catalytic system) suggested that gaseous oxygen dissolves dissociatively in LiCl, forming OCl^- as the active species on the chlorinated support, and then the decomposition of OCl^- produces oxygen and chlorine radicals, where both activate alkanes via homolytic hydrogen abstraction. The formed alkane radical reacts further with OH to form an appropriate alkene. The activity becomes higher by increasing Cl^- concentration but becomes limited by the availability of OCl^- diffusing through the molten layer [22].

Along with the increase in catalyst activity, increased selectivity has been observed as well. The higher selectivity was also found to be connected to the presence of the mentioned dynamic interface [24,25,27]. Ethene as the desired product is more stable via adsorption at the interface than the dissolved in liquid chloride, indicating that the interface plays an important role and the molten salt surface facilitates olefin desorption/release [14,16,18,24,25,29]. Moreover, molten salts prevent coke formation because the carbon floats on the surface of the melt where it could be skimmed off, which is a big problem in the traditionally supported metal oxide catalysts [2,7,8,30,31].

However, the unstable character of the supported alkali chloride systems has been observed and reported several times, but the reasons rely on the nature of the salts and supports [13–15,17,25–27,32,33]; therefore, more research studies are needed to clarify the ambiguous aspects. The varying degrees of retention of Cl^- suggest that the support material and its reaction with Cl^- are associated with the loss of chlorine. For metal oxide supports, it has been suggested that the formation of HCl causes deactivation over time in the materials prepared by chloride deposition. In MgO and MgO/Dy_2O_3, OH groups on the surface of the supports react with cations in the molten alkali chloride film, and the released H^+ forms dissolved HCl, which after enhancing the activity is depleted over time into the gas phase [27]. However, in another study for LiCl/MgO, a reaction between water and chlorine to produce HCl was suggested as the reason for the loss of chlorine, and water produced during the reaction promotes the loss of chlorine from the catalyst [34]. Even though it is not easy to detect HCl as an intermediate, a small amount of hydrogen chloride in the outlet was found during the ethane ODH reaction over metal chloride oxides consisting of bismuth, alkali, and alkaline earth chlorides [13]. Moreover, the chemical phase transformation along with the loss of chlorine that occurred during the reaction with alkali (Li, K, Na) chlorides/silica catalysts was reported to cause the deactivation together [15].

Preventing the loss of chlorine from the active catalyst might be very challenging because HCl is a likely intermediate in the reaction path and will tend to escape at high temperature [29]; thus, instead, regeneration was suggested by the addition of a Cl-containing compound [33]. Interesting research on ODH of ethane was done by using a set of various metal oxides in the presence of HCl in the gaseous feed, to avoid the loss of Cl^-, even though chlorine may cause corrosion problems. CeO_2-based catalysts exhibited the highest yield and besides, in the absence of HCl, CO_2 was the main product, but immediately upon increasing the partial pressure of HCl, the CO_x selectivity decreased sharply

and the selectivity to C_2H_4 increased, and the catalyst was stable over time [35]. In addition to using chlorine in the gaseous feed, the addition of chlorine in a catalyst as different alkali chlorides has been examined. The addition of $SrCl_2$ and KCl improved the catalytic yield of ethene by $SrBi_3O_4Cl_3$ expressively in the oxidative dehydrogenation of ethane, as is shown in Table 1 [13].

Recently, Ayari et al. [26] have reported an outstanding activity of binary and ternary mixtures of alkali and alkaline earth chlorides with the eutectic composition supported over lanthanum exchanged Na-Y zeolite in ODH of ethane. These catalysts were very active, the ethane conversion reached up to 40% with 100% selectivity to ethylene at relatively low temperature (500 °C) compared with other reported chloride-based systems mentioned above. Ayari's short communication reported a very interesting and new catalyst system capable of activating ethane at very low temperatures, but unfortunately, a more detailed characterization of the materials or information on the stability of these systems was not included in this communication.

Considering this introduction, it is evident that Cl-based catalysts are promising for ODH reaction; nevertheless, they suffer from deactivation. Thus, the long-term stability of the catalysts must be evaluated and knowledge about the deactivation mechanism could be useful for preparing the Cl-based catalyst with prolonged stability. Therefore, in this study, a binary eutectic mixture of KCl and $MgCl_2$ supported on La-FAU zeolite (supported alkali chlorides labaled as S-ACl), as one of the best representatives for alkali and alkaline earth chloride in Ayari's work [26], has been investigated as a catalyst for the ODH of ethane in more details with emphasis on the study of stability. This study brings detailed structural and compositional analysis of the pristine and spent catalysts, as well as information on catalyst stability and deactivation processes, kinetics, and character. Despite the promising short time activity and selectivity toward ethene, deactivation was found to be significant. The deactivation is connected with the loss of chlorine during the ODH reaction due to the formation of chlorinated hydrocarbons.

2. Results and Discussion

2.1. Catalytic Activity

In oxidative dehydrogenation of ethane, the catalyst reached the high initial ethane conversion of 80% after 15 min of feeding at 500 °C (see Table 1 and Figure 1). The oxygen is in great excess in the reaction mixture, so its conversion is only 8%, and thus, there is not any limitation for the conversion of ethane due to the lack of oxidizing reactants. Even though oxygen is in large excess, the main product is ethene with selectivity around 72%, while CO_2 and CH_4 selectivity was negligible (below 1%). No CO production was observed during the whole reaction.

According to the related reports in the literature, we can propose that a similar to well-known reaction mechanism [25,29,36] works in this system for ethylene formation, with an overall enthalpy of $\Delta_f H$ (298)= −105.5 kJ mol^{-1} [5].

$$KCl \leftrightharpoons K^+ + Cl^- / MgCl_2 \leftrightharpoons Mg^{2+} + 2Cl^- \quad (1)$$

$$\frac{1}{2} O_2 + Cl^- \leftrightharpoons OCl^- \quad (2)$$

$$OCl^- \leftrightharpoons O^- + Cl^\bullet / OCl^- \leftrightharpoons O^\bullet + Cl^- \quad (3)$$

$$O^\bullet + C_2H_6 \leftrightharpoons C_2H_5{}^\bullet + OH / Cl^\bullet + C_2H_6 \leftrightharpoons C_2H_5{}^\bullet + HCl \quad (4)$$

$$HCl + O^- \leftrightharpoons Cl^- + OH^\bullet \quad (5)$$

$$OH^\bullet + C_2H_5{}^\bullet \leftrightharpoons H_2O + C_2H_4 \quad (6)$$

$$\text{Overall reaction: } C_2H_6 + \frac{1}{2} O_2 \leftrightharpoons C_2H_4 + H_2O \quad (7)$$

Unfortunately, this exceptional low-temperature activity of the catalyst is not stable, as demonstrated by the conversions measured over the next 200 min on stream. The conversion of ethane declined sharply to ca. 22% after 45 min on the stream (Figure 1) and reduced to less than 10% after 100 min under the stream. The selectivity to ethene began to slowly increase to values around 91% under 206 min of time on the stream (TOS). The change in methane and CO_2 selectivity was kept below 3 and 5% during the reaction, but both slightly increased in selectivity. The measured activities of the FAU and La-FAU support exhibited negligible yield of 0.4 and 2.4%, respectively; thus, the observed activity is related to the catalytic system.

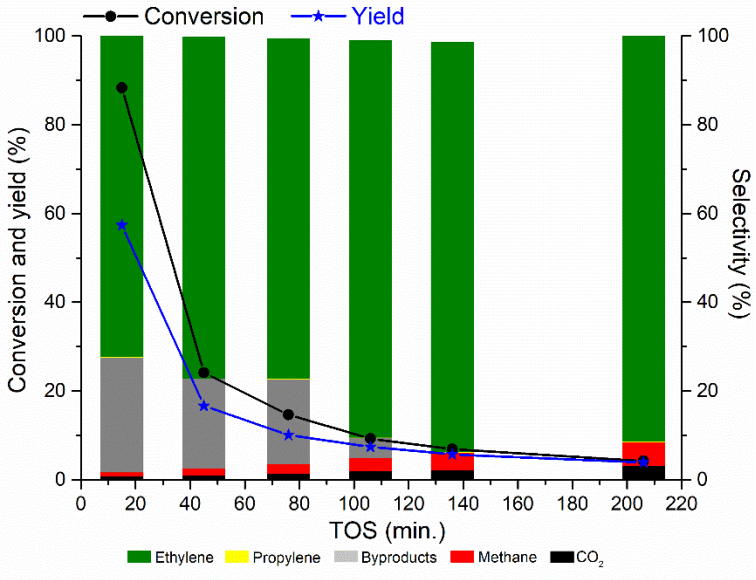

Figure 1. Conversion, yield, and selectivity dependence of ethane ODH as a function of time on stream for S-ACl.

Based on the carbon balance, we found that we are not able to analyze some of the products using gas chromatography (GC), because GC analysis was optimized for the determination of the main compounds of the reaction mixture (i.e., C_1–C_3 alkanes and alkenes, CO, CO_2, O_2, etc.). Missing reaction products based on gas chromatography analysis represented approximately 26% of selectivity at the initial period of the reaction and decreased to almost zero at 136 min of TOS. Therefore, the identification of the side products of the reaction generated on the surface of the catalyst is essential. Hence, the mass spectra of the outlet gases were measured in various times on stream. The mass spectra showed a fingerprint of the main products, as is ethylene, and water vapor accompanied by a low amount of CO_2 and methane. The presence of propane and propylene was detected as well with the selectivity below 1% (based on GC analysis) (Figure 2a). Molecular oxygen, ethane, and helium were detected also in large quantities. In addition to these major, and in gas chromatography detected substances, the species with a mass (m/z ratio) higher than 45 were detected in the effluent gas (Figure 2b). At low reaction time (TOS = 10 min), the mass signals at 49, 50, 52 62, 64, and 66 were clearly visible. The comparison of the experimental mass spectrum with reference mass spectra [37] resulted in that the peaks matched with m/z ratios 50, 62, and 64 correspond to chlorinated hydrocarbons comprising chloromethane, ethyl chloride, and chloroethene, respectively. A very low amount of HCl ($m/z = 36$), was also observed, perhaps playing an unstable intermediate role in the reaction formed by available Cl^- and H^+ from any source.

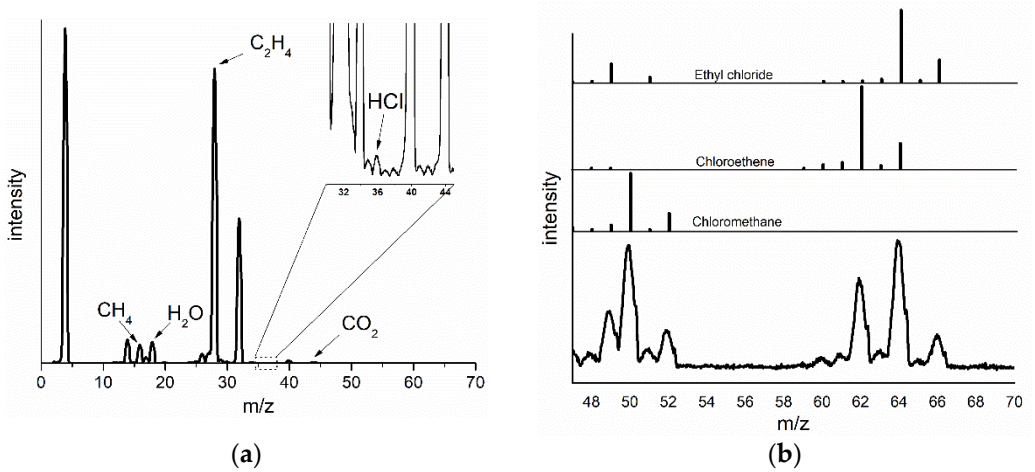

Figure 2. (**a**) Mass spectrum of the product of ethane oxidative dehydrogenation (ODH) over S-ACl, full-spectrum, and (**b**) details of low-intensity signals at m/z 45–70. At the bottom is displayed the experimental mass spectrum, above that are the model spectra of the three most probable chlorinated compounds formed during the reaction.

With increasing time on stream, the conversion of ethane decreased as well as the amount of side products. In addition, the nature of the side products changes, as can be seen in the changes of mass spectra character (Figure 3). Intensity of the main fragments of the chlorinated hydrocarbons disappeared during the first hour, and new signals at m/z = 45, 46, 47, 48, 68, and 84 were detected. These new by-products were comprised of some higher hydrocarbons (C_5) or oxygenates. The most possible compounds based on comparison with the reference mass spectra are allyl vinyl ether; 1,3-dimethylallene; trans-2-methyl-2-butenal; 2-methyl-2-butenal; 4-pentyne-2-ol; 3-butynoic acid; 2-buten-4-olide; 1-ethyl-2-methylacetylene; and 3-methyl-2-butenal [37].

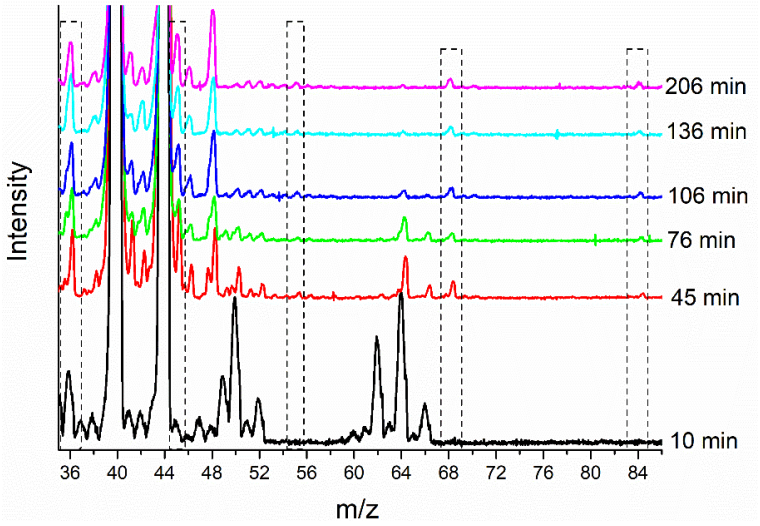

Figure 3. Mass spectra of the side products of ethane ODH over S-ACl during the reaction time including low-intensity signals at m/z 35–86.

Comparing the behavior of different catalytic systems reported in the literature is not entirely easy due to the use of often very different conditions. However, we tried to summarize the available data from the literature (Table 1). Chloride-based catalysts are very frequently studied in ethane ODH at temperatures higher than 500 °C, mostly 650 °C, and even higher [14,15,17,21,38]. The reported ethene yields for these works vary in a wide range from around 2 to 74%. Different alkali metals were exploited so far, for instance, Li [14,15,21,22,25,38], Na [13,25,26], K [13,16,25,26], Ba [17], Sr [13]. These alkali chlorides

have been used on various supports including silica, zirconia, Dy_2O_3, MgO, and other metal oxides. In general, different forms of zirconia as support exhibited higher activity and yields than the other supports. In all cases, the addition of chlorides resulted in higher activity and selectivity compared to pristine support. A similar catalyst as the one in this research was studied in Ayari's work, reporting 27% yield compared to 66% reported here for 15 min of TOS at the same temperature, although the time on stream for the measurements in Ayari's work is not mentioned. There are several reports on measuring at diverse longer TOS and higher temperatures [13,14,16,22,25], which have been compared with similar TOS in this research.

Table 1. Comparison of the catalyst's behavior in similar research with this study.

Catalyst	X *	S † (C_2H_4)	T #	Y ‡	TOS	Ref.
S-ACl	80	72	500	57	15	This work
NaY-La(Cl)-(NaMg)	2	100	500	2	-	[26]
NaY-La(Cl)-(KMg)	27	100	500	27	-	[26]
NaY-La(Cl)-(RbMg)	40	100	500	40	-	[26]
NaY-La(Cl)-(CsMg)	7	100	500	7	-	[26]
NaY-Bin(NaMg)	3	100	500	3	-	[26]
NaY-La(Cl)-(NaKMg)	20	100	500	20	-	[26]
$LiCl/SiO_2$	99	79	600	78	5	[15]
$NaCl/SiO_2$	88	69	550	61	5	[15]
KCl/SiO_2	70	75	550	52	5	[15]
LiCl/SZ (sulfated zirconia)	98	70	650	68	1	[14]
LiCl/AZ (amorphous zirconia)	87	60	650	52	1	[21]
LiCl/ZrON	95	71	650	68	1	[21]
LiCl/ZrOCl	28	97	650	27	1	[21]
LiCl/ZrSO4	89	83	650	74	1	[21]
LiCl/ SZ (sulfated zirconia)	53	90	650	48	1	[38]
$BaCl_2$–TiO_2–SnO_2	66	93	720	60	30	[17]
Li/Dy/Mg/O/C1	-	-	650	77	-	[22]
(Li-K)Cl-(Dy_2O_3/MgO) membrane	34	97	700	33	-	[16]
(Li-K)Cl-(Dy_2O_3/MgO) membrane	85	75	750	64	-	[16]
S-ACl	22	77	500	17	45	This work
$PbBi_3O_4Cl_3$	51	88	660	45	60	[13]
S-ACl	8	89	500	7	106	This work
Li/K/Cl-MgO/Dy_2O_3	5	94	550	5	120	[25]
Li/Na/Cl-MgO/Dy_2O_3	2	75	500	2	120	[25]
Li/Cl-MgO/Dy_2O_3	2	60	500	1	120	[25]
K/Cl-MgO/Dy_2O_3	2	40	500	1	120	[25]
Na/Cl-MgO/Dy_2O_3	2	37	500	1	120	[25]
S-ACl	4	91	500	4	206	This work
$SrBi_3O_4Cl_3$	20	89	660	17	360	[13]
$SrBi_3O_4Cl_3$ + $SrCl_2$	35	89	660	31	360	[13]
$SrBi_3O_4Cl_3$ + $2SrCl_2$	44	90	660	39	360	[13]
$SrBi_3O_4Cl_3$ + KCl	36	96	660	34	360	[13]
$SrBi_3O_4Cl_3$ + $SrCl_2$ + KCl	45	92	660	42	360	[13]
$SrBi_3O_4Cl_3$ + $SrCl_2$ + LiCl	42	94	660	40	360	[13]
$SrBi_3O_4Cl_3$ + $SrCl_2$ + NaCl	41	95	660	39	360	[13]
LiCl/ SZ (sulfated zirconia)	70	66	650	46	900	[14]

* Conversion (%), † Selectivity (%), # Temperature (∘C), ‡ Yield (%).

Among the systems reported in Table 1, $LiCl/SiO_2$ exhibited a large decrease in activity in a way that the conversion declined to 5% of the initial value after 15 h [15]. Exceptionally, LiCl supported on sulfated zirconia had been almost stable after 25 h under the stream [38], which contrasts with almost all other systems that exhibit deactivation in different trends.

2.2. Changes in the Catalyst during Pretreatment and ODH Reaction

To gain information about the changes of physico-chemical properties of the catalyst, the N_2 adsorption–desorption isotherms, scanning electron microscopy (SEM), energy-dispersive X-ray spectroscopy (EDX), and X-ray diffraction (XRD) were measured on the catalyst precursor, pretreated and spent catalysts (at various TOS). The prepared catalyst has shown different textural properties before and after the pretreatment as well as the ethane ODH reaction. The N_2 adsorption–desorption isotherms (Figure 4) of the zeolitic support and the mechanical mixture of the support and alkali chlorides have shown micro-porous features, whereas the fresh catalysts (after pretreatment by He, at 500 °C) and the spent catalysts have exhibited a non-porous character. The textural parameters of all measured samples obtained from N_2 adsorption isotherms are summarized in Table 2. The N_2 adsorption–desorption isotherms and textural properties of the pristine supports before and after the reaction showed no important differences, meaning any change in the textural properties of the catalyst is due to the presence of alkali chlorides. The difference in textural properties of the H-FAU before and after the reaction is due to the presence of carbon deposits after the reaction. It was proved by measuring N_2 adsorption–desorption isotherms of the spent H-FAU after calcination that exhibited similar textural properties to the fresh H-FAU before the reaction. The measured BET (Brunauer-Emmett-Teller) and external surface areas for the pristine support (La-FAU) were 450 and 8 m^2/g, respectively, with a pore volume of 0.19 cm^3/g. Considering the mass fraction of the La-FAU support in the catalyst, which was 50 wt%, and the fact that chlorides are non-porous materials with relatively large particle sizes, the textural properties of the physical mixture of La-FAU support with the eutectic mixture of $MgCl_2$ and KCl can be expected to be approximately equal to 50% of the values for the support in good agreement with the experimental results. The pretreatment of the mechanical mixture of support and alkali chlorides in helium flow at 500 °C (denoted as fresh catalyst), which is higher than the eutectic temperature of the mixture of alkali chlorides (473 °C) led to the chlorides melting and the formation of a uniform molten layer of salts on the support particles. Thus, the pretreated fresh catalyst exhibits non-porous character due to blocking of the entrance windows to the support pores by the molten salts layer, resulting in a drop of BET surface area to 7.7 m^2/g, which is a value very close to the external surface of the support particles. The N_2 adsorption isotherms of catalysts working under the reaction conditions for different times (Figure 2b) show that the textural properties of the catalyst are not influenced by the reaction and they correspond to the properties of the fresh catalyst (cf. data in Table 2).

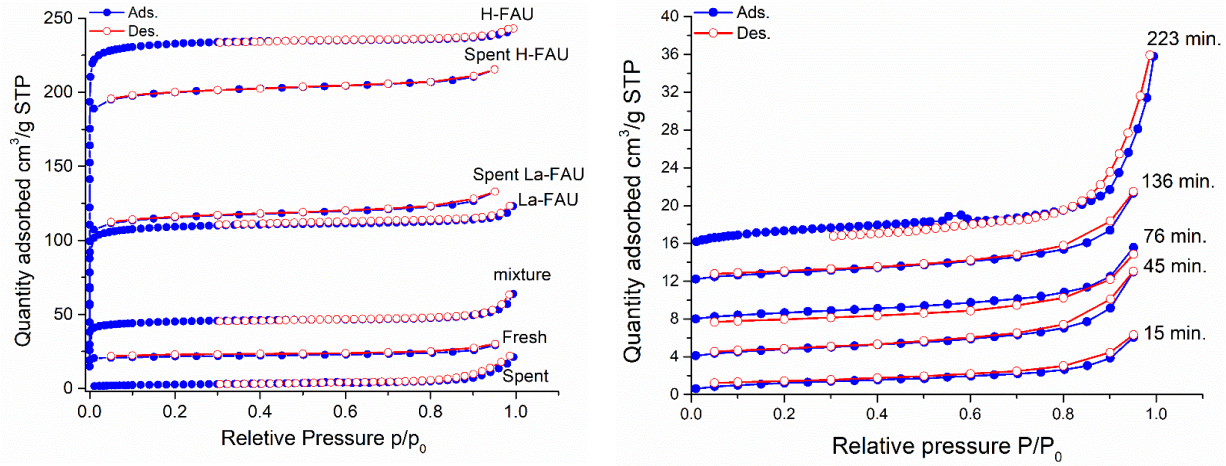

Figure 4. N_2 adsorption–desorption isotherms of (**a**) the fresh and spent pristine supports, physical mixture of S-ACl, the fresh catalyst before and after reaction (time on the stream (TOS): 223 min) in ethane ODH (isotherms corresponding to the fresh catalyst shifted along the y-axis by an increment of 20 cm^3/g), (**b**) the spent catalysts after different TOS under reaction atmosphere (isotherms are shifted along the y-axis by an increment of 4 cm^3/g).

Table 2. Textural properties of the support (La-FAU), mechanical mixture of S-ACl, fresh, and spent catalyst after the ethane ODH reaction in different TOS.

	S_{BET} (m^2/g) [a]	$S_{ext.}$ (m^2/g) [b]	$V_{mic.}$ (cm^3/g) [c]	V_p (cm^3/g) [d]
H-FAU	965	16	0.34	0.38
Spent H-FAU	769	16	0.30	0.33
La-FAU	450	8	0.17	0.19
Spent La-FAU	442	16	0.17	0.21
Mechanical mixture	179	4	0.07	0.10
Fresh	7.7	7.7	0	0.015
TOS: 15 min.	5.9	5.9	0	0.010
TOS: 45 min.	7.9	7.9	0	0.016
TOS: 76 min.	6.8	6.8	0	0.014
TOS: 136 min.	7.8	7.8	0	0.016
TOS: 223 min.	10	10	0	0.03

[a.] BET surface area, [b.] External surface area, [c.] Micropore volume, [d.] Total pore volume.

The SEM images of the parent FAU zeolite, La-FAU support, and fresh and spent catalysts under various time on stream are reported in Figure 5. The parent zeolite of the FAU structure exhibits polyhedral particles of ca. 500 nm in size. La-FAU support, fresh, and even spent catalysts exhibited no big difference in the morphology of the particles. It means that the zeolite support particles are quite stable and the molten salts form a surface layer on the external surface of the zeolitic support. Based on calculations, the thickness of the molten salts layer should be between 30 and 50 nm, according to the volume of the molten alkali chlorides (obtained from the related density) and the suggestion that the whole salt spreads over the external surface of the support or fills the micropores (by intrusion) and the rest of the salt spreads over the surface, respectively. If the whole external surface of the zeolite particles will be evenly covered, it does not cause any significant changes in the shape or size of the particles.

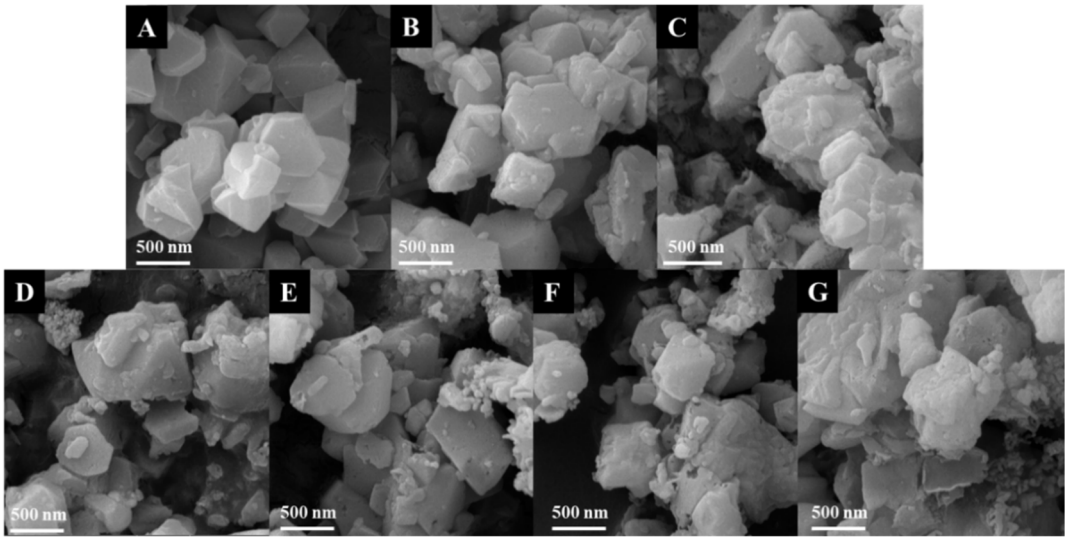

Figure 5. SEM images of (**A**) NH_4-FAU, (**B**) La-FAU, (**C**) Fresh catalyst, (**D**–**G**) Spent catalyst after 15, 45, 76, and 136 min under the reaction atmosphere, respectively.

The chemical composition of the materials investigated was determined by EDX spectroscopy. To obtain representative results, the composition was determined by averaging ten EDX measurements at different points of the sample on an area of at least 400 × 400 μm^2. Results (in atomic %) are summarized in Table 3. The parent NH_4-FAU zeolite has an Si/Al ratio of 2.55, and it is not changed with the preparation of catalysts and its working under reaction conditions for various TOS. La-FAU support prepared by solid-state reaction between NH_4-FAU and $LaCl_3$ exhibited an La/Al ratio of 0.52, which is slightly lower compared to the theoretical one (0.61), which can be ascribed to eventual partial sublimation, as was previously observed in the literature [39]. Surprisingly, the content of chlorine in the fresh catalyst after heat treatment at 500 °C in helium flow is ca. half compared to the theoretical expectation. We can speculate that during the heat treatment, the reaction between chlorides and moisture evaporated from the zeolite can lead to the partial conversion of chlorides to oxides. Nevertheless, the chlorine content has been reduced continuously during the reaction, decreasing from 11.5 to 6.3 at. %. At TOS = 223 min, almost 75% of chlorine is missing, but it seems that the content of chlorine levels off to approximately 25 rel.% of the original content. This part of chlorine is probably inaccessible from the surface (maybe inside the original zeolite channels) or is bound to more stable compounds. Simultaneously with the decrease in Cl content, an increase in oxygen content is noticeable. The content of alkali and alkaline earth metals remained almost constant.

Table 3. Chemical composition of S-ACl catalyst measured by energy-dispersive X-ray spectroscopy (EDX) based on the atomic percentage (at. %) of elements.

					Spent Catalysts, Different TOS (Min.)			
Element	**Nominal**	**NH_4-FAU**	**La-FAU**	**Fresh**	**15**	**45**	**76**	**136**	**223**
O	44.3	64.4	64.2	52.7	57.8	57.6	56.3	57.6	60.0
Na	0.1	1.4	1.1	0.7	0.9	0.9	0.7	0.7	0.7
Mg	8.3	0.0	0.0	9.4	11.6	10.4	13.1	13.2	9.7
Al	3.8	7.9	7.1	3.9	4.4	4.5	4.2	4.0	4.3
Si	9.8	20.2	17.9	9.1	11.1	11.4	10.8	10.4	11.8
Cl	24.3	0.0	5.9	11.5	11.1	7.6	7.1	6.6	6.3
K	7.6	0.0	0.0	5.8	5.5	5.2	5.4	5.1	5.4
La	1.7	0.0	3.7	1.7	2.6	2.5	2.4	2.5	1.9
N	0	6.1	0	0	0	0	0	0	0

X-ray diffraction patterns of the prepared catalyst exhibited the expected phases including FAU zeolite and alkali chlorides (Figure 6). According to the obtained XRD patterns, the mechanical mixture of the catalyst consists of crystalline KCl (Sylvite, Crystallography Open Database (COD) code: 9008651, lattice planes (002), (022) at 28.4° and 40.5°), $MgCl_2 \cdot 6H_2O$ (Bischofite, COD: 9011352, lattice planes (111), (310), (220), (11-2), (22-1) at 21.7°, 29.9°, 31°, 32.8°, and 33.9°, respectively), FAU zeolite (Faujasite, COD: 1507214, lattice planes (111), (022), (113), (133), (115), (044), (226), (137), (337) at 6.1°, 10°, 11.8°, 15.5°, 18.5°, 20.1°, 23.6°, 27.4°, and 29.3°, respectively), and LaOCl (Lanthanum–oxychloride, tetragonal, COD: 2101549, lattice planes (001), (011), (110), (012), and (020) at 12.8°, 25.2°, 30.7°, 33.9°, and 43.9°), meaning that the catalyst contains an excess of La; thus, not all La is in the cationic sites of zeolite and part of the lanthanum form oxychloride. Unlike KCl, the $MgCl_2$ showed a different crystalline structure ($MgCl_2 \cdot 6H_2O$, Bischofite) as its original form before mixing with the support. After the heat treatment at 500 °C, a solid solution of chlorides formed on the surface of the catalyst due to the dissolving of chlorides into each other; therefore, the changes in the quantity and intensity of the diffraction patterns are expected. The fresh catalyst exhibited the presence of FAU, LaOCl, and KCl, but not any form of $MgCl_2$ anymore. Furthermore, a new phase formed in the fresh catalyst, $LaAlO_3$ (lanthanum aluminum trioxide, COD: 2206576, lattice plane (011) at 33.4°). In the spent catalysts, besides LaOCl and KCl, SiO_2 (Cristobalite, COD: 9008233 (111) at 21.5°) is also present, whereas the presence of MgO (Periclase, COD: 9000501, lattice plane (002) at 42.9°) instead of its chloride form, showing the change in crystallinity after chlorine lost from the beginning of the reaction. It means that La-oxychloride and KCl are quite stable compounds, but $MgCl_2$ is highly labile. The intensity of the main diffraction line of FAU zeolite in low angles is decreased with time, which could be due to lowering its crystallinity. Additionally, the spent pristine support includes H-FAU and La-FAU have not exhibited important differences compared to the fresh ones, showing they are rather stable during the reaction.

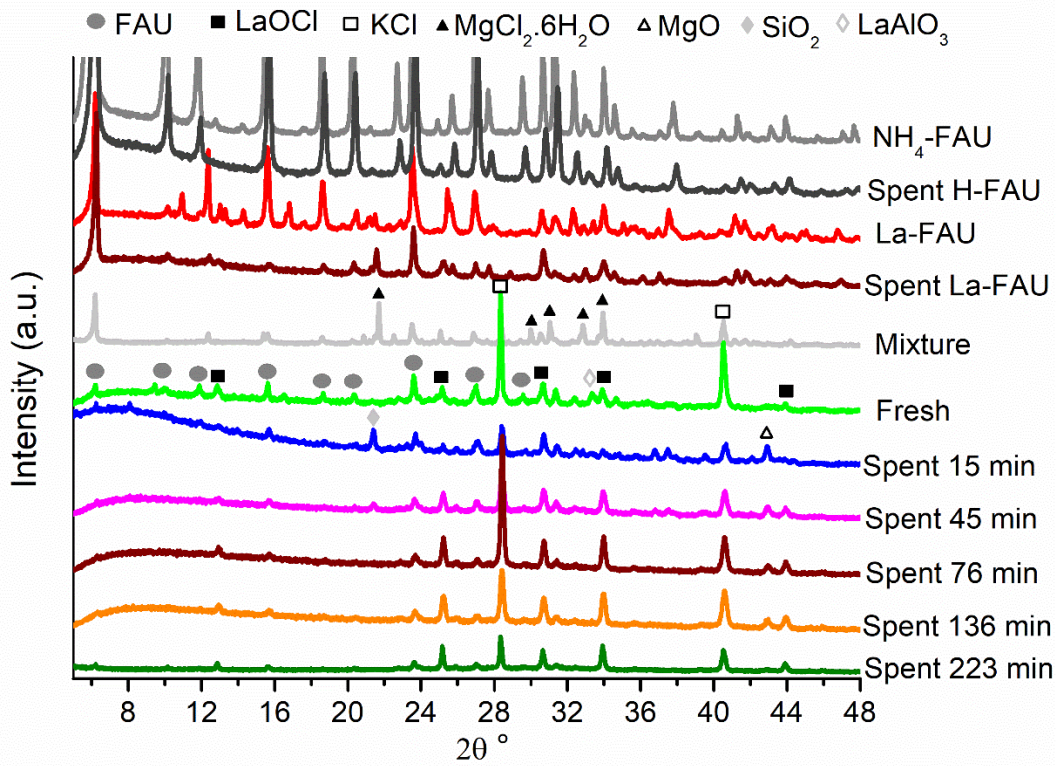

Figure 6. X-ray diffraction patterns of FAU-zeolite, La-FAU, as well as S-ACl catalyst before and after the ethane ODH reaction in TOS: 15, 45, 76, 136, and 223 min (patterns are shifted along the y-axis by an increment of 2500 a.u.).

3. Materials and Methods

3.1. Catalysts Preparation

The catalyst support (La-FAU) was prepared by solid-state ion exchange of 1 g NH_4-FAU zeolite (Zeolyst, Kansas City, KS, USA, Si/Al = 2.55) with 2 mmol $LaCl_3 \cdot 7H_2O$ (Sigma-Aldrich spol. s.r.o., Prague, Czech Republic). Precursors were mechanically mixed in an agate mortar and then were heated in an atmosphere control furnace by 2 °C min^{-1} heating rate to 500 °C for 12 h under N_2 flow (30 cm^3 min^{-1}). After that, the catalyst was prepared by extensively mixing KCl (Sigma-Aldrich spol. s.r.o., Prague, Czech Republic) and $MgCl_2$ (Sigma-Aldrich spol. s.r.o., Prague, Czech Republic), (mole fraction: 0.416 and 0.584, respectively, eutectic temperature: 473 °C) with La-FAU (salts-to-zeolite support mass ratio = 1:1) in an agate mortar. The mechanical mixture was converted to fresh catalyst just before the catalytic test (the material was heated in the flow of helium (27.3 cm^3 min^{-1}) to 500 °C with the heating rate 5 °C min^{-1} and kept at this temperature for 2 h). The catalyst is labeled S-ACl (supported alkali chlorides) in this study.

3.2. Catalytic Test

The catalytic activity of the sample for ethane ODH was tested in a plug-flow fixed-bed tubular reactor at atmospheric pressure. Typically, 200 mg of the catalyst was loaded in the glass tube reactor with an inner diameter of 5 mm (the grain size of the catalyst was between 0.35 to 0.5 mm). The pretreatment was performed at 500 °C by using 27.3 cm^3 min^{-1} of He for 2 h. Subsequently, the reaction was performed in a reaction mixture consisting of $C_2H_6/O_2/He$ = 3/15/82 vol % with a total flow of 33.33 cm^3 min^{-1} STP at 500 °C. Products were analyzed with an online gas chromatograph (Agilent 7890A, Agilent Corporation, Santa Clara, CA, USA) equipped with a flame ionization detector (FID) and a thermal conductivity detector (TCD) connected in series. The GS-Carbonplot GC column (60 m long with a diameter of 320 μm) was used for the separation of the gas mixture component. To analyze the essence of the by-products, a sample of gas products was collected at various time on stream into a glass sampling ampule and then analyzed by a quadrupole mass spectrometer OmniStar GDS 300 (Pfeiffer Vacuum, Aßlar, Germany).

3.3. Characterization

The catalyst support, fresh and spent catalysts were characterized by N_2 adsorption–desorption isotherms, XRD, and EDX/SEM. N_2 adsorption–desorption isotherms were measured at −196 °C, using an ASAP 2020 instrument. Before each adsorption measurement, the sample was degassed to allow a slow removal of pre-adsorbed water at low temperatures. The temperature was slowly increased with a temperature ramp of 0.5 °C min^{-1} up to 110 °C and evacuated at this temperature for 1 h; then, the temperature was increased with the rate of 1 °C min^{-1} until 250 °C was achieved. The sample was degassed at this temperature under a turbo molecular pump vacuum for 8 h. The surface area was obtained by using the BET model, the total volumes were estimated based on the adsorbed amount at a relative pressure of 0.99, micropore volume and external surface area were determined via the t-plot method employing a Harkins–Jura thickness curve. X-ray powder diffraction data were recorded on a Bruker D8 X-ray powder diffractometer equipped with a graphite monochromator and a position-sensitive detector (Vantec-1) using Cu Kα radiation (at 40 kV and 30 mA) in Bragg–Brentano geometry. The quantitative elemental composition of the catalysts was further evaluated using a scanning electron microscope (LYRA 3, Tescan, Brno-Kohoutovice, Czech Republic) equipped with EDX analyzer AZtec X-Max 20 (Oxford Instruments, Prague, Czech Republic) at an acceleration voltage of 20 kV. The morphology of particles in the sample was characterized by field emission scanning electron microscopy (LYRA 3, Tescan) at an acceleration voltage of 10 kV.

4. Conclusions

In this work, the catalytic activity and physico-chemical changes induced by ODH reaction in a binary eutectic mixture of KCl and $MgCl_2$ supported on La-FAU zeolite as

one of the best representatives for alkali and alkaline earth chloride catalysts reported previously by Ayari's group has been studied. This catalytic system exhibits high activity, as well as high selectivity in a short time on the stream, and a negligible formation of CO_2. Yield of the ethene reached up to 65%. The changes that occurred on the catalyst were studied and disclosed that the interaction between the formed molten layer and feed changed the properties of the catalyst over time, including porosity, phase content, and chemical composition. Loss of catalyst activity in TOS is associated with the loss of chlorine from the catalyst evidenced by EDX analysis of catalysts working in the reaction for various times. It is surprising that the loss of chlorine was observed even during high-temperature treatment in helium, which was very probably due to the reaction of desorbed water vapor with the chlorides. XRD analysis evidenced that $MgCl_2$ is more prone to exchange chlorine for oxygen. Chlorine is removed from the catalyst in the form of chlorinated hydrocarbons such as chloromethane, ethyl chloride, and chloroethene. Surprisingly, the exchange of chlorine for oxygen occurs not only under catalytic reaction but also under the helium flow, which was probably due to the reaction of chlorides at high temperature with traces of water vapor desorbed from the zeolite support. It indicates high lability of the catalyst. As chlorine is the crucial element to form hypochlorite anions, subsequently, a dropping in the amount of available active species happens. It is interesting that approximately 25 rel.% of chlorine remained in the catalyst even after 223 min in the reaction. This part of chlorine is probably inaccessible from the surface (maybe inside the original zeolite channels) or is bound to more stable compounds (probably KCl or LaOCl). It means that activity of the catalyst is tightly connected with the presence of $MgCl_2$. We believe that this research clarifies an obstacle in the discussed catalytic system, and it is a step forward to find the solution to build an appropriate catalyst.

Author Contributions: Conceptualization, R.B. and M.S.; methodology, M.S.; validation, R.B., M.S., and S.Š.; formal analysis, M.S.; investigation, M.S. and S.Š.; data curation, M.S.; writing—original draft preparation, M.S.; writing—review and editing, R.B.; visualization, M.S.; supervision, R.B.; All authors have read and agreed to the published version of the manuscript.

Funding: This research was funded by University of Pardubice, grant number "SGS_2021_006".

Data Availability Statement: Publicly available datasets were analyzed in this study. These data can be found here: DOI: https://doi.org/10.18434/T4D303, and http://www.crystallography.net/cod/ (accessed on 18 March 2021).

Acknowledgments: This work was supported by the Ministry of Education, Youth, and sports with financial support under project No. SGS_2021_006. The SEM and EDX facilities at CEMNAT institute were employed in this study with financial support under project No. LM2018103. Ludvík Beneš was kindly acknowledged for helping XRD measurements.

Conflicts of Interest: The authors declare no conflict of interest. The funders had no role in the design of the study; in the collection, analyses, or interpretation of the data; in the writing of the manuscript, or in the decision to publish the results.

References

1. James, O.O.; Mandal, S.; Alele, N.; Chowdhury, B.; Maity, S. Lower alkanes dehydrogenation: Strategies and reaction routes to corresponding alkenes. *Fuel Process. Technol.* **2016**, *149*, 239–255. [CrossRef]
2. Sattler, J.J.H.B.; Ruiz-Martinez, J.; Santillan-Jimenez, E.; Weckhuysen, B.M. Catalytic Dehydrogenation of Light Alkanes on Metals and Metal Oxides. *Chem. Rev.* **2014**, *114*, 10613–10653. [CrossRef] [PubMed]
3. Blasco, T.; Galli, A.; Nieto, J.L.; Trifiró, F. Oxidative Dehydrogenation of Ethane andn-Butane on VOx/Al2O3Catalysts. *J. Catal.* **1997**, *169*, 203–211. [CrossRef]
4. Ciambelli, P.; Lisi, L.; Pirone, R.; Ruoppolo, G.; Russo, G. Comparison of behaviour of rare earth containing catalysts in the oxidative dehydrogenation of ethane. *Catal. Today* **2000**, *61*, 317–323. [CrossRef]
5. Gärtner, C.A.; van Veen, A.C.; Lercher, A.J. Oxidative Dehydrogenation of Ethane: Common Principles and Mechanistic Aspects. *ChemCatChem* **2013**, *5*, 3196–3217. [CrossRef]
6. Gärtner, C.A.; Van Veen, A.C.; Lercher, J.A. Oxidative Dehydrogenation of Ethane on Dynamically Rearranging Supported Chloride Catalysts. *J. Am. Chem. Soc.* **2014**, *136*, 12691–12701. [CrossRef] [PubMed]

7. Bañares, M.A. Supported metal oxide and other catalysts for ethane conversion: A review. *Catal. Today* **1999**, *51*, 319–348. [CrossRef]
8. Cavani, F.; Ballarini, N.; Cericola, A. Oxidative dehydrogenation of ethane and propane: How far from commercial implementation? *Catal. Today* **2007**, *127*, 113–131. [CrossRef]
9. Carrero, C.; Schlögl, R.; Wachs, I.; Schomaecker, R. Critical literature review of the kinetics for the oxidative dehydrogenation of propane over well-defined supported vanadium oxide catalysts. *ACS Catal.* **2014**, *4*, 3357–3380. [CrossRef]
10. Navalon, S.; Dhakshinamoorthy, A.; Alvaro, M.; Garcia, H. Carbocatalysis by Graphene-Based Materials. *Chem. Rev.* **2014**, *114*, 6179–6212. [CrossRef]
11. Ronghe Lin, A.P.A.; Pérez-Ramírez, J. Halogen-Mediated Conversion of Hydrocarbons to Commodities. *Chem. Rev.* **2017**, *117*, 4182–4247.
12. Burch, G.D.S.R.; Tsang, S.C. Comparative study of catalysts for the oxidative coupling of methane. *Appl. Catal. A Gen.* **1988**, *43*, 105–116. [CrossRef]
13. Ueda, W.; Lin, S.-W.; Tohmoto, I. Highly selective oxidative dehydrogenation of ethane to ethene over layered complex metal chloride oxide catalysts. *Catal. Lett.* **1997**, *44*, 241–245. [CrossRef]
14. Wang, S.; Murata, K.; Hayakawa, T.; Hamakawa, S.; Suzuki, K. Lithium-chloride-promoted sulfated zirconia catalysts for the oxidative dehydrogenation of ethane. *Catal. Lett.* **1999**, *59*, 173–178. [CrossRef]
15. Wang, S.; Murata, K.; Hayakawa, T.; Hamakawa, S.; Suzuki, K. Oxidative Dehydrogenation of Ethane over Alkali Metal Chloride Modified Silica Catalysts. *Energy Fuels* **2000**, *14*, 899–903. [CrossRef]
16. Li, M.; van Veen, A.C. Selective production of ethylene via continuous oxidative dehydrogenation of ethane in (Dy2O3/MgO)-(Li-K) Cl composite membrane reactor. *Chem. Eng. J.* **2019**, *365*, 344–350. [CrossRef]
17. Wang, Z.; Chen, L.; Zou, G.; Luo, X.; Gao, R.; Chou, L.; Wang, X. A novel $BaCl_2$–TiO_2–SnO_2 catalyst for the oxidative dehydrogenation of ethane. *Catal. Commun.* **2012**, *25*, 45–49. [CrossRef]
18. Kristoffersen, H.H.; Metiu, H. Molten LiCl Layer Supported on MgO: Its Possible Role in Enhancing the Oxidative Dehydrogenation of Ethane. *J. Phys. Chem. C* **2015**, *119*, 8681–8691. [CrossRef]
19. Zichittella, G.; Lüthi, J.; Paunović, V.; Pérez-Ramírez, J. Alkane Functionalization via Catalytic Oxychlorination: Performance as a Function of the Carbon Number. *Energy Technol.* **2020**, *8*. [CrossRef]
20. Wang, D.J.; Rosynek, M.P.; Lunsford, J.H. The effect of chloride ions on a li+-mgo catalyst for the oxidative dehydrogenation of ethane. *J. Catal.* **1995**, *151*, 155–167. [CrossRef]
21. Wang, S.; Murata, K.; Hayakawa, T.; Suzuki, K. Oxidative Dehydrogenation of Ethane over Zirconia-Supported Lithium Chloride Catalysts. *Chem. Eng. Technol.* **2000**, *23*, 1099–1103. [CrossRef]
22. Gaab, S.; Find, J.; Grasselli, R.; Lercher, J. Oxidative ethane activation over oxide supported molten alkali metal chloride catalysts. In *Catalyst Deactivation, Proceedings of the 7th International Symposium, Edinburgh, UK, 24–25 May 2004*; Elsevier: London, UK, 2004; Volume 147, pp. 673–678.
23. Yuan, X.H.; Zhao, Y.B.; Jin, Y.X.; Weng, W.Z.; Wan, H.L. Oxidative dehydrogenation of ethane to ethylene over $LiCl/SO_4^{2-}$-ZrO_2 catalyst. *Chin. J. Catal.* **2006**, *27*, 79–85.
24. Tope, B.; Zhu, Y.; Lercher, J.A. Oxidative dehydrogenation of ethane over Dy_2O_3/MgO supported LiCl containing eutectic chloride catalysts. *Catal. Today* **2007**, *123*, 113–121. [CrossRef]
25. Kumar, C.P.; Gaab, S.; Muller, T.E.; Lercher, J.A. Oxidative Dehydrogenation of Light Alkanes on Supported Molten Alkali Metal Chloride Catalysts. *Top. Catal.* **2008**, *50*, 156–167. [CrossRef]
26. Ayari, F.; Charrad, R.; Asedegbega–Nieto, E.; Mhamdi, M.; Delahay, G.; Farhat, F.; Ghorbel, A. Ethane Oxidative Dehydrogenation over ternary and binary mixtures of alkaline and alkaline earth chlorides supported on zeolites. *Microporous Mesoporous Mater.* **2017**, *250*, 65–71. [CrossRef]
27. Gärtner, C.A.; Van Veen, A.C.; Lercher, J.A. Highly Selective Supported Alkali Chloride Catalysts for the Oxidative Dehydrogenation of Ethane. *Top. Catal.* **2014**, *57*, 1236–1247. [CrossRef]
28. Kristoffersen, H.H.; Metiu, H. Chemistry of Solvated Electrons in Molten Alkali Chloride Salts. *J. Phys. Chem. C* **2018**, *122*, 19603–19612. [CrossRef]
29. Gaab, S.; Machli, M.; Find, J.; Grasselli, R.; Lercher, J. Oxidative Dehydrogenation of Ethane Over Novel Li/Dy/Mg Mixed Oxides: Structure–Activity Study. *Top. Catal.* **2003**, *23*, 151–158. [CrossRef]
30. Grant, J.T.; Venegas, J.M.; McDermott, W.P.; Hermans, I. Aerobic Oxidations of Light Alkanes over Solid Metal Oxide Catalysts. *Chem. Rev.* **2018**, *118*, 2769–2815. [CrossRef]
31. Bulánek, R.; Čičmanec, P.; Sheng-Yang, H.; Knotek, P.; Čapek, L.; Setnička, M. Effect of preparation method on nature and distribution of vanadium species in vanadium-based hexagonal mesoporous silica catalysts: Impact on catalytic behavior in propane ODH. *Appl. Catal. A: Gen.* **2012**, *415–416*, 29–39. [CrossRef]
32. Zichittella, G.; Aellen, N.; Paunović, V.; Amrute, A.P.; Pérez-Ramírez, J. Olefins from Natural Gas by Oxychlorination. *Angew. Chem. Int. Ed.* **2017**, *56*, 13670–13674. [CrossRef] [PubMed]
33. Leveles, L.; Fuchs, S.; Seshan, K.; Lercher, J.A.; Lefferts, L. Oxidative conversion of light alkanes to olefins over alkali promoted oxide catalysts. *Appl. Catal. A: Gen.* **2002**, *227*, 287–297. [CrossRef]
34. Conway, S.J.; Lunsford, J.H. The oxidative dehydrogenation of ethane over chlorine-promoted lithium-magnesium oxide catalysts. *J. Catal.* **1991**, *131*, 513–522. [CrossRef]

35. Yu, F.; Wu, X.; Zhang, Q.; Wang, Y. Oxidative dehydrogenation of ethane to ethylene in the presence of HCl over CeO_2-based catalysts. *Chin. J. Catal.* **2014**, *35*, 1260–1266. [CrossRef]
36. Gaab, S.; Find, J.; Muller, T.E.; Lercher, J.A. Kinetics and mechanism of the oxidative dehydrogenation of ethane over Li/Dy/Mg/O/(Cl) mixed oxide catalysts. *Top Catal.* **2007**, *46*, 101–110. [CrossRef]
37. NIST Mass Spectrometry Data Center, W.E.W. Director, "Mass Spectra". In *NIST Chemistry WebBook*; NIST Standard Reference Database Number, 69; Linstrom, P.J., Mallard, W.G., Eds.; National Institute of Standards and Technology: Gaithersburg, MD, USA, 2005; p. 20899. retrieved March 18, 2021. [CrossRef]
38. Wang, S.B.; Murata, K.; Hayakawa, T.; Hamakawa, S.; Suzuki, K. Performance of metal-oxide-promoted LiCl/sulfated-zirconia catalysts in the ethane oxidative dehydrogenation into ethene. *Catal. Lett.* **1999**, *62*, 191–195. [CrossRef]
39. Schüßler, F.; Pidko, E.A.; Kolvenbach, R.; Sievers, C.; Hensen, E.J.M.; Van Santen, R.A.; Lercher, J.A. Nature and Location of Cationic Lanthanum Species in High Alumina Containing Faujasite Type Zeolites. *J. Phys. Chem. C* **2011**, *115*, 21763–21776. [CrossRef]